

INTERNATIONAL SOCIETY FOR SOIL MECHANICS AND GEOTECHNICAL ENGINEERING



This paper was downloaded from the Online Library of the International Society for Soil Mechanics and Geotechnical Engineering (ISSMGE). The library is available here:

<https://www.issmge.org/publications/online-library>

This is an open-access database that archives thousands of papers published under the Auspices of the ISSMGE and maintained by the Innovation and Development Committee of ISSMGE.

Overconsolidation effects on secondary compression rates

Effets de la surconsolidation sur les taux de consolidation secondaire

E.Alonso, A.Lloret, A.Gens & M.Salvado – Technical University of Catalunya, Barcelona, Spain

ABSTRACT: The secondary compression behaviour of a reconstituted low plasticity clay has been investigated. Oedometer tests performed included loading, unloading and reloading sequences. In this way the effect of OCR, loading increment ratio and the intensity of the final reloading or creeping stress was determined. It was found that, once the soil is overconsolidated ($OCR \geq 1.5$), the secondary compression deformations depend on the loading increment ratio and the current creeping stress. A working model for secondary compression strains, which incorporates the experimental findings, was developed. Secondary deformations are proportional to the primary deformations associated with the loading increment ratio and to a function of time, which is controlled by the intensity of the reloading stress. Model predictions and actual measurements are in good agreement for a significant number of tests characterised by widely different stress sequences.

RÉSUMÉ: Dans cet article, le comportement en compression secondaire d'une argile reconstituée de faible plasticité est étudié sur la base d'essais oedométriques comportant des séquences de chargement, déchargement et rechargement. Il apparaît que, une fois le sol surconsolidé ($OCR \geq 1.5$), les déformations de compression secondaire dépendent du rapport d'incrément de charge et de l'état actuel de contrainte de fluage. Ces résultats ont conduit au développement d'un modèle qui incorpore les effets précédemment cités. Les déformations secondaires y sont proportionnelles aux déformations primaires associées aux rapport d'incrément de charge et à une fonction du temps contrôlée par l'intensité de la contrainte de rechargement. Une bonne concordance entre les prédictions du modèle et les mesures expérimentales a été obtenue pour un nombre significatif d'essais réalisés sous des séquences de chargement très différentes.

1 INTRODUCTION

Preloading is a well-established procedure to reduce settlements of structures founded on soft clay soils. Primary settlements are in general easily controlled if the design foundation stresses do not exceed the applied preloading stress. In sensitive structures, however, or when the foundation soils exhibit a marked long-term settlement, secondary effects are relevant. Field and laboratory experience (Ladd 1971, Mesri 1973, Koutsoftas et al 1987, Yu and Frizzi 1994) have shown that overconsolidating the soil has a remarkable effect in reducing secondary compression rates. In a recent study involving a long-term instrumented preloading tests on deltaic deposits (Alonso et al 2000), strain rates determined in the field were shown to depend on the estimated "in situ" overconsolidation ratio. Figure 1 shows this dependence. The soil profile was Normally Consolidated (NC) in the upper 10-15 m and the OCR gradually increased with depth to a maximum value close to 1.4 at 60 m depth. The figure also shows the approximate linear relationship between deformation rate and time when both are in log scale. Also plotted in the figure are the rates of secondary settlements determined in a number of consolidation tests, which will be examined in more detail in this paper.

In the test program performed, reconstituted samples of the foundation deltaic clays were subjected to the stress path sketched in Figure 2. The stress paths reproduce a situation that is often encountered in practice. The soil is first loaded and then unloaded (stresses σ'_c and σ'_u). This stage corresponds to the preloading treatment of the soil. When the structure is built, a final reloading (σ_r in Fig. 2) is applied. Three different stress levels (σ'_c , σ'_u , σ'_r) may be identified, in general, in a preloading foundation problem. In the tests described in this paper secondary settlements were recorded at constant σ_r whereas the stress history (initial state $\rightarrow \sigma'_c \rightarrow \sigma'_u \rightarrow \sigma'_r$) was performed at a relatively fast rate, ensuring, however, the dissipation of excess pore water pressures at the reference stress points.

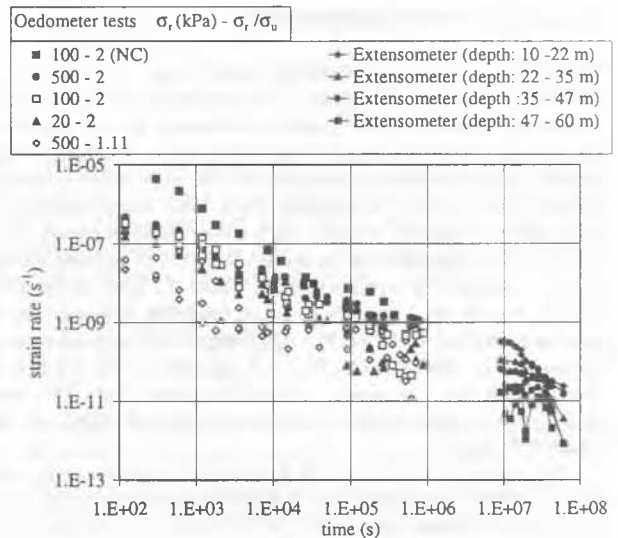


Figure 1. Secondary compression rates measured "in situ" and in the laboratory.

The strain rates recorded in laboratory tests are plotted in Figure 1 for different values of the final σ'_r stress and the stress ratio σ'_r/σ'_u . They seem to be consistent with the field records if the different time scales of each set of observations is taken into account. This is an encouraging result, which adds confidence to the research performed in the laboratory. The aim of this investigation is to find improved models for secondary consolidation when the history of unloading-reloading is introduced.

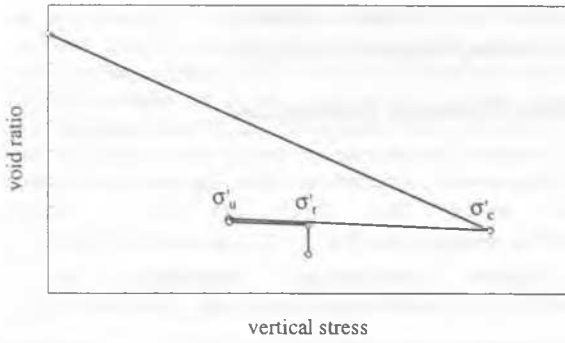


Figure 2. Definition of the stress sequence applied to specimens.

Table 1. Experimental program.

σ'_c (kPa)	σ'_u (kPa)	σ'_r (kPa)	σ'_r / σ'_u	σ'_c / σ'_r
50	50	100	2	0.5
30				1.5
40	10	20	2	2
100				5
150				1.5
200	50	100	2	2
500				5
1500				15
750				1.5
1000	250	500	2	2
1500				3
750				1.5
1000	450	500	1.11	2
2500				5

2 LABORATORY EXPERIMENTS

The soil used is a low plasticity deltaic clay (CL, ML: $w_L = 40.1\%$; $w_p = 24.9\%$; $\% < 2\mu m : 13\%$) from the Llobregat delta in Barcelona. Samples were initially recovered at the site of the future waste water treatment plant of the city. Additional information on the in situ characteristics of the clay may be found in Alonso et al 2000). Specimens were then reconstituted to a common void ratio ($e = 0.85$) under a low effective stress ($\sigma'_v = 10$ kPa). The experimental program, in terms of the applied σ'_c , σ'_u , σ'_r stresses, is synthesised in Table 1. Two stress ratios (σ'_r / σ'_u and σ'_c / σ'_r) are also given in the table. The ratio σ'_c / σ'_r may be identified as the OCR at the time of the long-term test (at constant σ'_r). The ratio (σ'_r / σ'_u) is a measure of the intensity of the loading step previous to the long-term test. The loading/unloading paths cover a wide range of void ratios, as indicated in Figure 3.

The value of (σ'_c / σ'_r), or OCR, for all tests performed, except one, is equal to or larger than 1.5. In one occasion only, a normally consolidated sample ($\sigma'_c = 50$ kPa; $\sigma'_u = 50$ kPa; $\sigma'_r = 100$ kPa) was tested. The investigation reported here essentially refers to samples that have undergone a moderate or significant overconsolidation ($OCR \geq 1.5$).

The strain time history under σ'_r of all the samples tested is shown in Figure 4. Each test is identified by a triad ($\sigma'_c \sigma'_u \sigma'_r$). The deformations plotted in figure 4 correspond to a secondary behaviour of the soil. In order to facilitate the comparison among different cases, an initial strain, which corresponds to a common time $t = 120$ s, is subtracted from results in Figure 5. A detailed examination of Figure 5 reveals that the different strain histories tend to concentrate into clusters of similar behaviour. Largest delayed strains develop for specimens that have the largest σ'_r / σ'_u ratio although the influence of the absolute value of σ'_r is also noticeable. The value of OCR ($= \sigma'_c / \sigma'_r$) does not seem to control the secondary strain rate in a significant way. It should

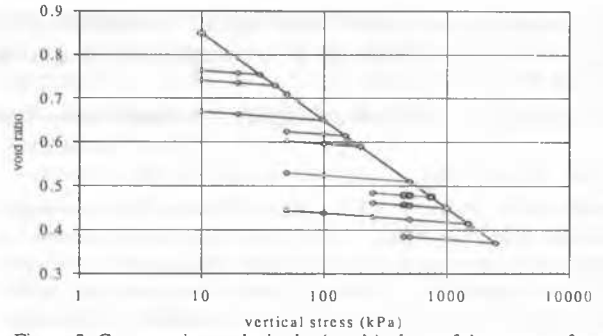


Figure 3. Compression paths in the (e, σ'_v) plane of the tests performed.

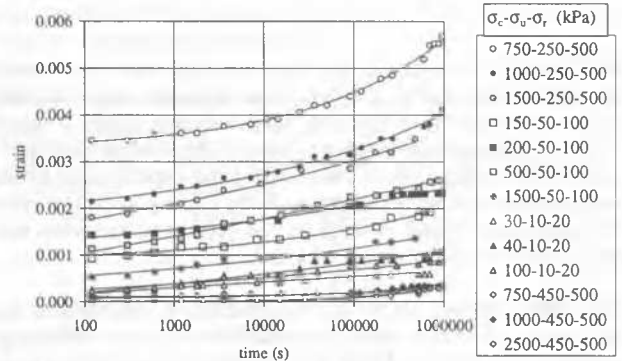


Figure 4. Secondary compression deformations of all samples tested ($OCR \geq 1.5$).

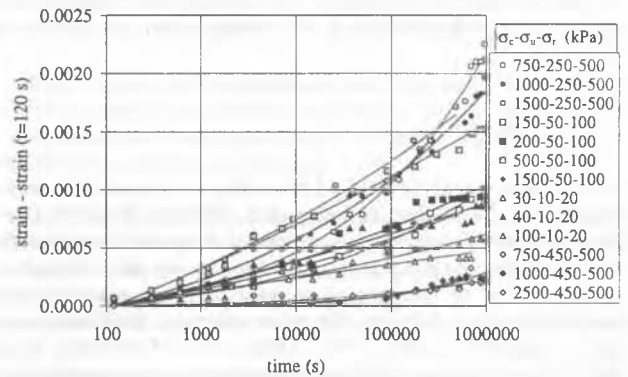


Figure 5. Secondary compression deformations in excess of the measured early deformation at $t = 120$ s ($OCR \geq 1.5$).

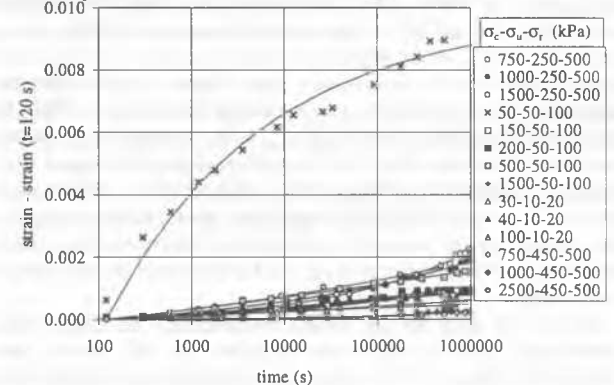


Figure 6. Secondary compression rates for all samples tested.

be stressed however that all the cases plotted in Figure 5 correspond to $OCR \geq 1.5$. In fact, if the specimen with OCR is included (Fig. 6), a different picture arises. What Figure 5 indicates is that OCR has not a definite influence on long-term creep behaviour provided $OCR \geq 1.5$.

Strain rates were computed on the basis of results presented in Figure 4 (or 5). A moving average, which includes 5 successive

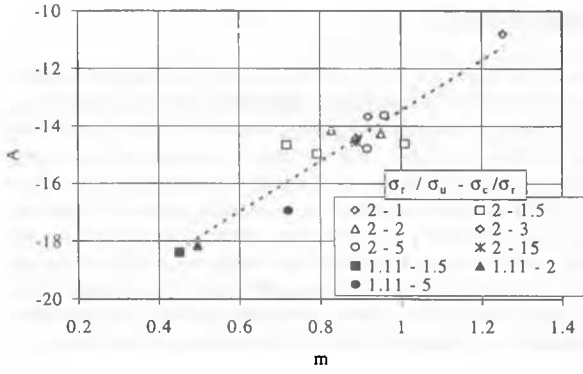


Figure 7. Correlation observed between parameters A and m .

recorded points, was used to reduce the instability of the numerical derivative. The computed strain rates were already shown in Figure 1, against in situ strain rates.

3 MODELLING SECONDARY STRAINS

3.1 Secondary strain rates

Figure 1 suggests, a $\dot{\epsilon}$ was already advanced by Mitchell (1981), that the strain rate decays with time in such a way that the strain rate and time, both in log scale, are linearly related:

$$\log \dot{\epsilon} = \log \dot{\epsilon}_i - m \log t / t_i \quad (1)$$

where ϵ_i is a reference strain rate for $t = t_i$ and m is the slope of the relationship (m is a positive number). Integration of equation (1) between an initial strain (ϵ_i for $t = t_i$) and a generic strain ϵ for time t leads to the following secondary strain model:

$$\epsilon = \epsilon_i + \frac{\dot{\epsilon}_i t_i}{1-m} \left[\left(\frac{t}{t_i} \right)^{1-m} - 1 \right], \quad (2)$$

an equation which is slightly different from the expression proposed by Mitchell. If $m = 1$, integration of equation (1) leads to:

$$\epsilon = \epsilon_i + \dot{\epsilon}_i t_i \ln t / t_i \quad (3)$$

which is the classical expression for secondary compression strains. Equation (3) is the limiting value of equation (2) as $m \rightarrow 1$. In the remaining of the paper only the general expression (2) will be used.

In equation (2), ϵ_i may be interpreted as a model parameter. If $\log \epsilon = A$, equation (2) has two parameters: A and m . A describes the initial rate of secondary deformation, whereas m provides an indication of the evolution of strain rate with time.

The measured strain histories (Fig. 4, 5 and 6) indicate that A and m are far from being constant for a given soil. They depend on σ'_c , σ'_u and σ'_r . Expression (2) was fitted to the measured results. In this way, pairs (A, m) were found for all the tests performed. It was found that A and m are correlated (Fig. 7): a faster initial rate of secondary deformations imply a higher m value. This is a convenient result, in the sense that it reduces "de facto" the material parameters of equation (2). However, the relationship between m (or A) and the stress history should be investigated.

3.2 Influence of loading history on secondary compression rates

Consider first the effect of the stress increment ratio σ'_r/σ'_n . Results for a common σ'_r ($\sigma'_r = 500$ kPa) and two different values of σ'_r/σ'_u (2 and 1.1) are plotted in Figure 8. The effect of the size of the loading increment is clearly shown. The figure sug-

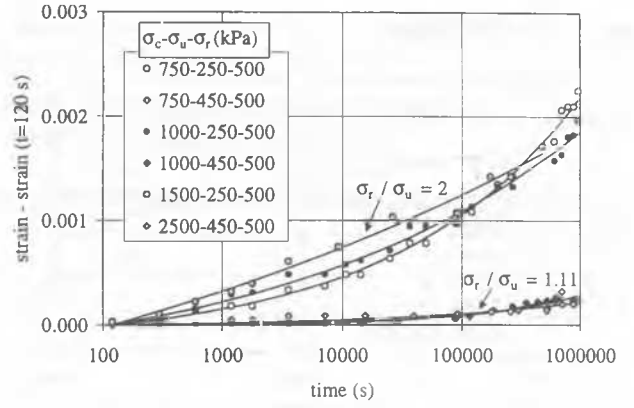


Figure 8. Influence of stress ratio on secondary compression deformations.

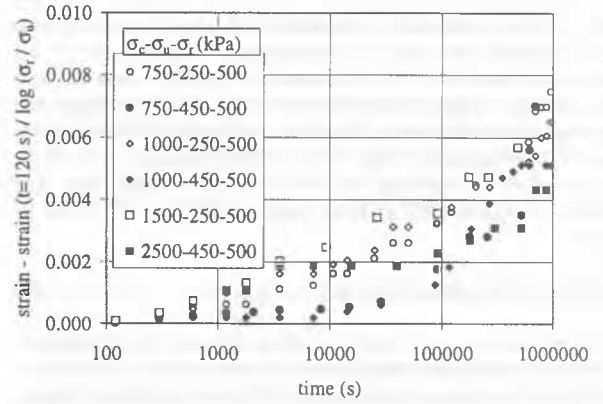


Figure 9. Normalised values of secondary compression.

gests the following normalisation of equation (2):

$$\Delta \epsilon = \epsilon - \epsilon_i = \log \left(\frac{\sigma'_r}{\sigma'_u} \right) \frac{e^A t_i}{1-m} \left[\left(\frac{t}{t_i} \right)^{(1-m)} - 1 \right] \quad (4)$$

The term $\log(\sigma'_r/\sigma'_u)$ is related to the primary settlements ϵ^p when the load increment is applied ($\log \sigma'_r/\sigma'_u = \epsilon_p (1+e) / C_s$, where e is the current void ratio and C_s the compression index. In a normally consolidated case C_s should be substituted by C_c). Therefore, the model for secondary strains becomes:

$$\Delta \epsilon = \frac{\epsilon_p (1+e)}{C_s} \frac{e^A t_i}{1-m} \left[\left(\frac{t}{t_i} \right)^{(1-m)} - 1 \right] \quad (5)$$

This form of the equation stresses that the secondary deformation depends on the amount of primary compression.

If Equation (4) or (5) is applied to the data shown in Figure 8, the variability is largely reduced as shown in Figure 9. Consider now the effect of the absolute value of σ'_r , i.e. the "creeping" stress. Strain histories for a common stress increment ratio $\sigma'_r/\sigma'_u = 2$ and different values of σ'_r were collected in Figure 5. Three groups of strain histories are identified. They correspond, in decreasing order of accumulated strain, to $\sigma'_r = 20, 100$ and 500 kPa. Some discrepancies may be found but the trend is clearly marked. The plot suggests that parameter m should be related to the absolute value of the applied stress σ'_r . The correlation found between m and σ'_r for different values of σ'_r/σ'_u is given in Figure 10. A least square fit is given by the equation:

$$m = 1.31 - 0.094 \ln \sigma'_r \quad (6) \quad 4 \text{ CONCLUSIONS}$$

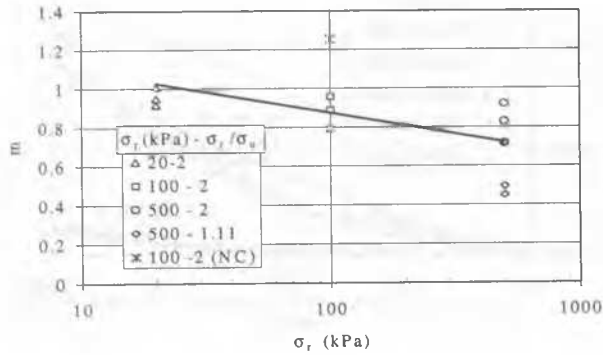


Figure 10. Correlation observed between model parameter m and applied stress.

This empirical relationship, together with equation (3), essentially completes the model for secondary compression of the Barcelona deltaic clay. It is expected that different clays will exhibit different relationship between material parameter m and the reloading or creeping stress (Equation (6)) and a different correlation between m and A (Fig. 7). It is believed however, that the basic structure of Equation (4) or (5) will be maintained. The structure of equation (5) is better appreciated if it is written as follows:

$$\Delta \varepsilon(t) = f_1(\varepsilon_p) f_2(A) f_3(t) \quad (7)$$

In this equation $f_1(\varepsilon_p) = \varepsilon_p (1+e)/C_s = \log(\sigma'_r/\sigma'_v)$ introduces the effect of stress increment ratio. The function $f_2(A) = e^A = \varepsilon_i$ provides the effect of the initial strain rate and finally, function $f_3(t) = t^{1-m} [(t/t_i)^{1-m} - 1]$ describes the evolution in time of secondary deformation. The effect of the intensity of applied stress (σ'_r) is found in m , through its correlation with σ'_r and also in function $f_2(\varepsilon_i)$ since A and m seem to be strongly correlated. For the tests performed, for which $OCR \geq 1.5$, an improved adjustment was found for a function $f_2(A)$ slightly modified:

$$f_2(A) = ae^{A(m)} = 3.3 e^{(16.1-1.96m)} \quad (8)$$

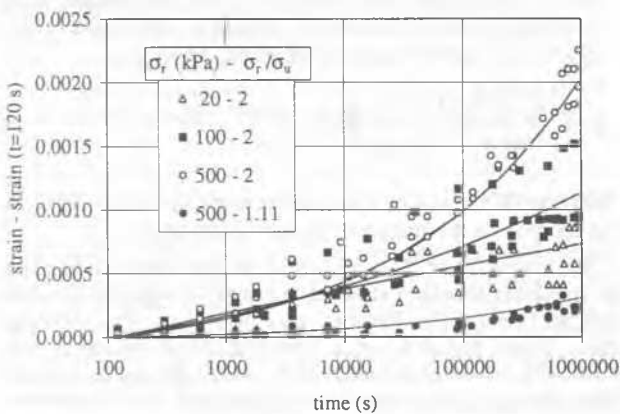


Figure 11. Comparison between model predictions and measured secondary compression strains.

A comparison between measured strain histories and model predictions, based on Equation (7) and (8) is shown in Figure 11 for the four cases considered, in terms of stress increment ratio ($\sigma'_r/\sigma'_v = 1.11$ and 2) and creeping stress ($\sigma'_r = 20, 100$ and 500 kPa). All cases considered in Figure 11 correspond to $OCR \geq 1.5$. The agreement, which is satisfactory, demonstrates the capabilities of the model proposed to predict secondary compression strains.

Preloading techniques to improve soft soil deformation characteristics lead often to a loading stage along the NC compression line, a partial unloading and a final reloading under foundation design loads. This sequence has been simulated in an experimental program. The purpose of this investigation was to derive improved models for secondary consolidation strains. It has been argued that secondary compression deformations become frequently a critical issue in preloading design especially when sensitivity structures are founded on soft clays. The model developed may be helpful when accurate models of secondary compression are required. Most of the results reported here correspond to overconsolidation ratios in excess of 1.5.

It has been found that secondary compression rates (in logarithmic scale) measured for every combination of unloading and reloading stresses may be expressed as a linear function of the logarithm of time. This is a result already reported (Mitchell, 1981). However, the material parameters of this law are far from being constant and they have been shown to vary, in a significant way, with the reloading or creeping stress. Moreover, measured secondary deformations are proportional to the previous primary deformations experienced during the application of the reloading stage. These findings have led to the development of a comprehensive secondary compression model under confined (oedometric) conditions. The secondary strain increment was expressed as the product of three contributions, or factors:

1. The primary consolidation strain corresponding to the applied stress increment.
2. A function that is a measure of the initial secondary strain rate.
3. A function of time.

The second and third function essentially depend on the absolute value of the reloading stress. Model parameters have been identified for the low plasticity (CL-ML) deltaic clay tested. The agreement between predicted secondary strain histories and measured ones for different combinations of stress increment ratio and reloading or creeping stress was found very satisfactory.

5 REFERENCES

- Alonso EE, Gens A & Lloret A (2000) Precompression design for secondary settlement reduction. *Géotechnique* 50(6): 645-656.
- Ladd CC (1971) *Settlement analysis of cohesive soils*. Research Report R71-2. Cambridge, MA: MIT.
- Mesri G (1973) Coefficient of secondary compression. *J. Soil Mech. Found. Div. ASCE* 99(1): 123-137.
- Mitchell JK (1981) *Fundamentals of soil behaviour*. Wiley.
- Koutsoftas DC, Fott R & Handfelt LD (1987) Geotechnical investigations offshore Hong Kong. *J. Geotech. Engng. Div. ASCE* 113(2): 87-105.
- Yu KP & Frizzi RP (1994) Preloading organic soils to limit future settlements. In *Vertical and horizontal displacements of foundations and embankments*. ASCE Geotechnical Special Publication. 40(1): 476-490.